Autonomous Motorcycles for Agile Maneuvers, Part I: Dynamic Modeling

Jingang Yi, Yizhai Zhang, and Dezhen Song

***Abstract*— Single-track vehicles, such as motorcycles, provide an agile mobile platform. Modeling and control of motorcycles for agile maneuvers, such as those by professional racing riders, are challenging due to motorcycle's unstable platform and complex tire/road interaction. As a first step attempting to understand how racing riders drive a motorcycle, in this two-part paper we present a modeling and tracking control design of an autonomous motorcycle. In this first-part paper, we discuss a new dynamics model for the autonomous motorcycle. We consider the existence of lateral sliding velocity at each wheel contact point. Because of the importance of the tire/road interaction for vehicle stability and maneuverability, the dynamic modeling scheme also includes the motorcycle tire models. The new nonlinear dynamic models are used for control systems design in the companion paper with control input variables are the front wheel steering angle and the angular velocities of front and rear wheels.**

NOMENCLATURE

X, Y, Z	A ground-fixed coordinate system.
x, y, z	A wheel-base line moving coordinate system.
x_w, y_w, z_w	A front wheel plane coordinate system.
x_B, y_B, z_B	A rear frame body coordinate system.
C_1, C_2	Front and rear wheel contact points on the ground.
F_{fx}, F_{fy}, F_{fz}	The front wheel contact forces in the x, y, z-axis directions.
F_{rx}, F_{ry}, F_{rz}	The rear wheel contact forces in the x, y, z directions.
$\boldsymbol{v}_f, \boldsymbol{v}_r$	Velocity vectors of the front and rear wheel contact points, respectively.
v_{fx}, v_{fy}	Front wheel contact point C_1 velocities along the x- and y-axis directions, respectively.
v_{rx}, v_{ry}	Rear wheel contact point C_2 velocities along the x- and y-axis directions, respectively.
v_{fx_w}, v_{fy_w}	Front wheel contact point C_1 velocities along the x_w- and y_w-axis directions, respectively.
v_X, v_Y	Rear wheel contact point C_2 velocities along the X- and Y-axis directions, respectively.
ω_f, ω_r	Wheel angular velocities of the front and rear wheels, respectively.
$\boldsymbol{v}_G$	Velocity vector of the motorcycle frame (with rear wheel set).
γ_f, γ_r	Slip angles of the front and rear wheels, respectively.
λ_f, λ_r	Longitudinal slip values of the front and rear wheels, respectively.
φ, ψ	Rear frame roll and yaw angles, respectively.
φ_f	The front steering wheel plane camber angle.
ϕ	Motorcycle steering angle.
ϕ_g	Motorcycle kinematic steering angle (projected steering angle on the ground plane).
σ	The front kinematic steering angle variable.
m	The total mass of the motorcycle rear frame and wheel.
J_s	The mass moment of rotation of the steering fork (with the front wheel set) about its rotation axis.
l	Motorcycle wheel base, i.e., distance between C_1 and C_2.
l_t	The front steering wheel trail.
h	The height of the motorcycle center of mass.
r	The front and rear wheel radius.
δ	The rear frame rotation angle from its vertical position.
ξ	The front steering axis caster angle.
R	The radius of the trajectory of point C_2 under neutral steering turns.
C_d	The aerodynamics drag coefficient.
k_λ, k_γ, k_φ	Longitudinal, lateral, and camber stiffness coefficients of motorcycle tires, respectively.
$L(L_c)$	The (constrained) Lagrangian of the motorcycle systems.

This work is supported in part by the National Science Foundation under grant CMMI-0856095.

J. Yi is with the Department of Mechanical and Aerospace Engineering, Rutgers University, Piscataway, NJ 08854 USA. E-mail: jgyi@rutgers.edu.

Y. Zhang is with the Department of Information and Communication Engineering, Xi'an Jiaotong University, Xi'an 710049, Shaanxi Province, P.R. China.

D. Song is with the Department of Computer Science and Engineering, Texas A&M University, College Station, TX 77843 USA. E-mail: dzsong@cse.tamu.edu.

I. INTRODUCTION

Single-track vehicles, such as motorcycles and bicycles, have high maneuverability and strong off-road capabilities. In environments such as deserts, forests, and mountains, mobility of single-track vehicles significantly outperforms that of double-track vehicles. The recent demonstration of the Blue Team's autonomous motorcycle (Fig. 1(a)) in the 2005 DARPA Grand Challenge autonomous ground vehicles competition has shown an example of the high-agility of the single-track platform [1].

Although the extensive study of the motorcycle dynamics have revealed some knowledge of motorcycle platform under

Preprint submitted to 48th IEEE Conference on Decision and Control.
Received March 5, 2009.

steady motions, however, modeling and control of motorcycles for agile maneuvers, such as those by professional racing riders, still remains a challenging task due to motorcycle's intrinsic unstable platform and complex tire/road interaction. Professional motorcycle riders can leverage the safety limits of the tire/road interaction, and maintain the vehicles at high performance while preserving safety. Understanding how human drivers carry out these maneuvers not only advances our knowledge in vehicle dynamics and control, but also can be used for enhancing vehicle safety, such as designing new driver assistance systems, for example, emergency obstacle avoidance maneuvers.

(a) (b)

Fig. 1. (a) The Blue team autonomous motorcycle. (b) A Rutgers autonomous pocket bike.

As a first step towards to to understand such high-performance capabilities of the human drivers, and then design human-inspired control algorithms for agile maneuvers, the objective of this two-part paper is to develop a new modeling and control scheme for an autonomous motorcycle. Comparing with existing study on the motorcycle dynamics and control, the main contribution of this study is the new modeling and control system design with integrated motorcycle dynamics with tire/road interaction. First, we do not enforce a zero lateral velocity nonholonomic constraint for the wheel contact points of the motorcycle system. Such nonholonomic constraints are not realistic for high-fidelity vehicle modeling [2]. Second, we explicitly consider the tire/road interaction for designing control algorithms because of the importance of the tire/road interaction on motorcycle dynamics. To our knowledge, there is no study that explicitly considers such kinds of tire dynamics into the motorcycle control system design. Based on the new dynamics, in our companion paper [3], we extend the control system design in [4], [5] for trajectory following maneuvers.

The remainder of the paper is organized as follows. We review some related work in Section II. In Section III, we discuss dynamic modeling of a riderless motorcycle. In Section IV, we present a motorcycle tire dynamics model and then integrate the tire dynamics with the motorcycle dynamics. Finally, we conclude the paper in Section V.

II. Related Work

Mathematically modeling of a bicycle or a motorcycle has been an active research area for many years. Although some modeling differences have been discussed in [2], from control system design aspects, we consider bicycles and motorcycles are similar, and hence do not explicitly distinguish them. There is a large body of work that studies motorcycle stability and dynamics, and readers can refer to two recent review papers: one from a historical development viewpoint [2] and the other from a control-oriented perspective [6].

The modeling work can be considered as two groups [6]: a simple inverted pendulum model and a multi-body dynamic model. For example, some simple second-order dynamic models are presented in [7] to study the balance stability of a bicycle. Several researchers have studied the motorcycle dynamics using multi-body dynamics [8]–[11]. The model developed in [9] is very comprehensive and contains various vehicle components. The model has been implemented in a simulation package called *FastBike* for the purposes of real-time simulations. Multi-body dynamics models are not suitable for the control system design due to their complexity while a inverted-pendulum model overly simplify the problem and does not capture all of the dynamics and geometric characteristics.

In [4], [12], mathematical models of a motorcycle are discussed using (constrained) Lagrange's equations. In [13], experimental study of the motorcycle handling is compared with the mathematical dynamics model of a motorcycle with the rider. Stability and steering characteristics of a motorcycle are typically discussed using a linearization approach with a consideration of a constant velocity [2], [6], [8], [14]–[17]. A *non-minimum phase* property (unstable poles and zeros in motorcycle dynamics) in these analyses explains the counter-steering phenomena and other steering stability observations. In [14], it is also demonstrated experimentally the in-significance of the gyroscopic effect of the front wheel.

The concept of an autonomous bicycle without a rider has been proposed by several researchers [1], [4], [5], [18]–[21]. In this two-part paper, we extend the modeling and control design in [4], [5]. For the modeling part, we take a constrained Lagrangian approach to capture the nonlinear dynamics of a motorcycle. Besides the consideration of control-oriented modeling approach that captures the fundamental properties of the motorcycle platform with a manageable complexity, several new features have been adopted and developed. First, we relax the zero lateral velocity of the wheel contact points and therefore allow wheel sliding in the models, which provides more realistic vehicle modeling [2]. Second, we explicitly consider the tire/road interaction for designing control algorithms because of the importance of the tire/road interaction on motorcycle dynamics [22]. The study in [23] is probably the closest work to ours. The authors in [23] employ a nonholonomic motorcycle dynamics and focus on the performance and maneuverability analysis of motorcycles using the automotive tire/road interaction characteristics.

III. Motorcycle Dynamics

Fig. 1(b) shows the Rutgers autonomous motorcycle prototype. The motorcycle is rear-wheel driving. Steering and velocity control are considered as control inputs for the riderless autonomous motorcycle. We do not consider the weight shifting as one actuation mechanism as human drivers

Preprint submitted to 48th IEEE Conference on Decision and Control.
Received March 5, 2009.

because the Blue Team motorcycle has previously demonstrated an effective maneuverability only through vehicle steering and velocity control [1].

A. Geometry and kinematics relationships

The riderless motorcycle is considered as as a two-part platform: a rear frame and a steering mechanism. Fig. 2(a) shows a schematic of the vehicle. We consider the following modeling assumptions: (1) the wheel/ground is a point contact and thickness and geometry of the motorcycle tire are neglected; (2) The motorcycle body frame is considered a point mass; and (3) the motorcycle moves on a flat plane and vertical motion is neglected, namely, no suspension motion.

We denote C_1 and C_2 as the front and rear wheel point points with the ground, respectively. As illustrated in Fig. 2(a), three coordinate systems are used: the navigation frame $\mathcal{N}$ (X, Y, Z-axis fixed on the ground), the wheel base moving frame (x, y, z-axis fixed along line C_1C_2), and the rear body frame $\mathcal{B}$ (x_B, y_B, z_B-axis fixed on the rear frame). For the frame $\mathcal{B}$, we use (3-1-2) Euler angles and represent the motion by the yaw angle ψ and roll angle φ. We denote the unit vector sets for the three coordinate systems as $(\boldsymbol{I}, \boldsymbol{J}, \boldsymbol{K})$, $(\boldsymbol{i}, \boldsymbol{j}, \boldsymbol{k})$, and $(\boldsymbol{i}_B, \boldsymbol{j}_B, \boldsymbol{k}_B)$, respectively. It is straightforward to obtain that

$$\begin{bmatrix} \boldsymbol{i}_B \\ \boldsymbol{j}_B \\ \boldsymbol{k}_B \end{bmatrix} = \left[\begin{array}{c:c} 1 & \mathbf{0} \\ \hdashline \mathbf{0} & \boldsymbol{R}(\varphi) \end{array}\right] \begin{bmatrix} \boldsymbol{i} \\ \boldsymbol{j} \\ \boldsymbol{k} \end{bmatrix} = \left[\begin{array}{c:c} 1 & \mathbf{0} \\ \hdashline \mathbf{0} & \boldsymbol{R}(\varphi) \end{array}\right] \left[\begin{array}{c:c} \boldsymbol{R}(\psi) & \mathbf{0} \\ \hdashline \mathbf{0} & 1 \end{array}\right] \begin{bmatrix} \boldsymbol{I} \\ \boldsymbol{J} \\ \boldsymbol{K} \end{bmatrix}$$
$$= \begin{bmatrix} \mathrm{c}_\psi & \mathrm{s}_\psi & 0 \\ -\mathrm{c}_\varphi \mathrm{s}_\psi & \mathrm{c}_\varphi \mathrm{c}_\psi & \mathrm{s}_\varphi \\ \mathrm{s}_\varphi \mathrm{s}_\psi & -\mathrm{s}_\varphi \mathrm{c}_\psi & \mathrm{c}_\varphi \end{bmatrix} \begin{bmatrix} \boldsymbol{I} \\ \boldsymbol{J} \\ \boldsymbol{K} \end{bmatrix}, \tag{1}$$

where the rotation matrix

$$\boldsymbol{R}(x) = \begin{bmatrix} \mathrm{c}_x & \mathrm{s}_x \\ -\mathrm{s}_x & \mathrm{c}_x \end{bmatrix}$$

and $\mathrm{c}_x := \cos x$, $\mathrm{s}_x := \sin x$ for angle x.

We consider the trajectory of the rear wheel contact point C_2, denoted by its coordinates (X, Y) in $\mathcal{N}$, as the motorcycle position. The orientation of the coordinate systems and the positive directions for angles and velocities follow the conversion of the SAE standard [17].

We consider the instantaneous rotation center of the motorcycle motion on the horizontal plane. Let O_r denote the instantaneous rotation center and O_r' denote the neutral instantaneous rotation center which is the intersection point of the perpendicular lines of the front and rear wheel planes; see Fig. 2. Under the neutral turning condition [10], the slip angles of the front and rear wheels are the same, that is, $\lambda_f = \lambda_r$, and then the rotation center angles for O_r and O_r' are equal to the kinematic steering angle ϕ_g, namely, $\alpha = \alpha' = \phi_g$. Let R denote the instantaneous radius of the trajectory of point C_2 under neutral turning conditions. We define σ as the kinematic steering variable as

$$\sigma := \tan\phi_g = \frac{l}{R}. \tag{2}$$

From the geometry of the front wheel steering mechanism [10], we find the following relationship,

$$\tan\phi_g \, \mathrm{c}_\varphi = \tan\phi \, \mathrm{c}_\xi \ . \tag{3}$$

If we assume a small roll and steering angles, then from (3) we obtain an approximation

$$\dot{\sigma} \, \mathrm{c}_\varphi = \dot{\phi} \, \mathrm{c}_\xi \, . \tag{4}$$

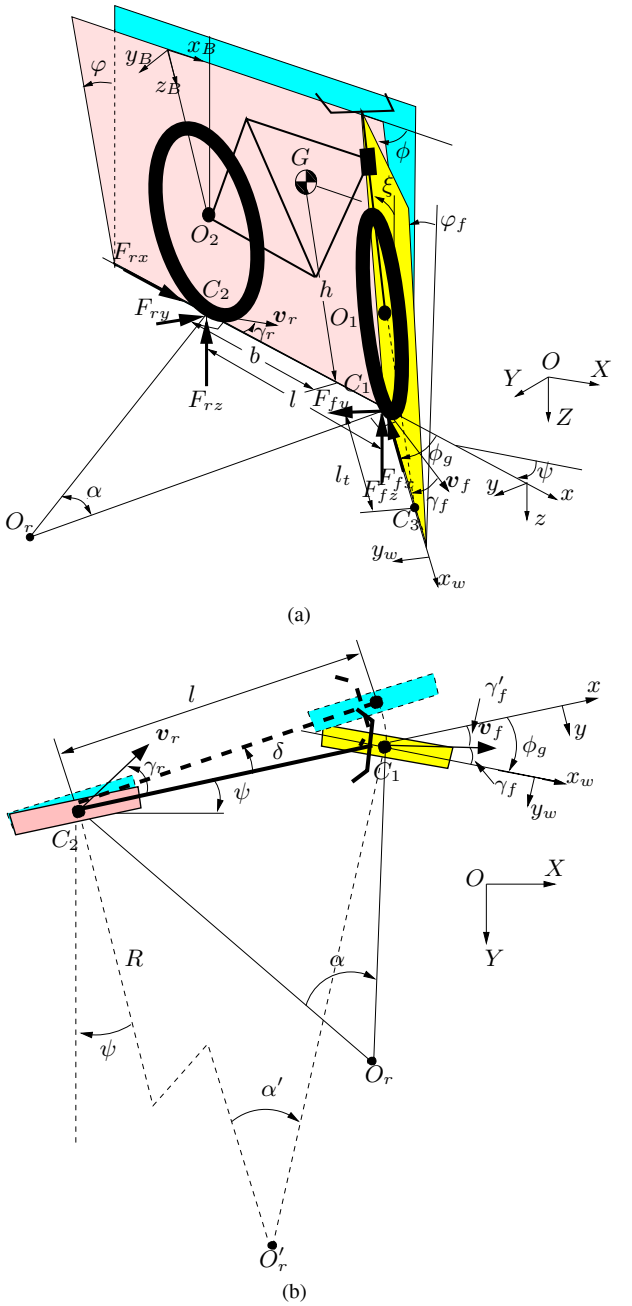

Fig. 2. A picture of the Blue team autonomous motorcycle [1].

The motion of the motorcycle on the XY plane can be captured by the generalized coordinates $(X, Y, \psi, \varphi, \sigma)$. Note that the use of variable σ is to capture the steering impact on the motorcycle dynamics. The nonholonomic constraint of the rear wheel and the motion trajectory geometry imply the yaw kinematics equality

$$v_{rx} = R\dot{\psi} = \frac{l}{\sigma}\dot{\psi} \, . \tag{5}$$

From a differential geometry viewpoint [1], we can partition

[1]We here take a description of the base-fiber structure of nonholonomic dynamical systems with symmetry in [24].

Preprint submitted to 48th IEEE Conference on Decision and Control.
Received March 5, 2009.

the generalized velocities of the motorcycle as base velocities $\dot{\boldsymbol{r}} = [\dot{\varphi},\, v_{rx},\, v_{ry},\, \dot{\sigma}]^T$ and fiber velocities $\dot{\boldsymbol{s}} = \dot{\psi}$. We then write the constraints in (5) simply as

$$\dot{\boldsymbol{s}} + A(\boldsymbol{r}, \boldsymbol{s})\dot{\boldsymbol{r}} = 0, \tag{6}$$

where $A(\boldsymbol{r}, \boldsymbol{s}) = \begin{bmatrix} 0 & -\frac{\sigma}{l} & 0 & 0 \end{bmatrix}$.

Due to the steering mechanism and caster angle, the height of the mass center of gravity of the motorcycle is changing under steering. As shown in Fig. 2(b), the height change Δh_G of the center of gravity G due to the steering action can be calculated as [5]

$$\Delta h_G = \delta b \, \mathrm{s}_\varphi \approx \frac{b l_t \sigma \, \mathrm{c}_\xi}{l} \, \mathrm{s}_\varphi \,, \tag{7}$$

where we use a small angle approximation $\sigma \approx \phi_g$ from the relationship (2).

Remark 1: In [4], [23], the steering axis is assumed to be vertical. This assumption simplifies the motorcycle dynamics and neglects a significant geometric stabilization mechanism, which is the "motorcycle trail" (denoted as l_t in Fig. 2(a)) discussed in [7], [10], [14], [15]. The resulting model of the motorcycle dynamics cannot capture the influence of the steering angle ϕ on the roll dynamics when $v_{rx} = 0$. Namely, one cannot use steering to stabilize the motorcycle. Such an observation is also pointed out in [6].

Given the roll angle φ and the steering angle ϕ, the camber angle of the front wheel can be approximated as [10]

$$\varphi_f = \varphi + \phi \, \mathrm{s}_\xi \,. \tag{8}$$

We consider the relationship between velocities of the rear wheel contact point C_2 and the front wheel center O_1. We write the position vector $\boldsymbol{r}_{O_1} = \boldsymbol{r}_{C_2} + \boldsymbol{\rho}_{C_2O_1}$, where $\boldsymbol{r}_{C_2}$ is the position vector of point C_2 and $\boldsymbol{\rho}_{C_2O_1} = l\boldsymbol{i}_B - r\boldsymbol{k}_B = l\boldsymbol{i} + r\,\mathrm{s}_\varphi \boldsymbol{j} - r\,\mathrm{c}_\varphi \boldsymbol{k}$ is the relative position vector of G. The angular velocity of the rear frame is represented as $\boldsymbol{\omega} = \dot{\varphi}\boldsymbol{i} + \dot{\psi}\boldsymbol{k}$. Thus, we obtain

$$\begin{aligned} \boldsymbol{v}_{O_1} = \dot{\boldsymbol{r}}_{C_2} + \boldsymbol{\omega} \times \boldsymbol{\rho}_{C_2O_1} = (v_{rx} - r\dot{\psi}\,\mathrm{s}_\varphi)\boldsymbol{i} + \\ (v_{ry} + l\dot{\psi} + r\dot{\varphi}\,\mathrm{c}_\varphi)\boldsymbol{j} + r\dot{\varphi}\,\mathrm{s}_\varphi\,\boldsymbol{k}. \end{aligned} \tag{9}$$

B. Motorcycle dynamics

We use the constrained Lagrangian method in [24] to obtain the dynamics equation of the motion of the riderless motorcycle. We consider the motorcycle as two parts: one rear frame with mass m and one steering mechanism with the mass moment of inertia J_s. The Lagrangian L of the motorcycle is calculated as

$$L = \frac{1}{2}J_s\dot{\phi}^2 + \frac{1}{2}m\boldsymbol{v}_G \cdot \boldsymbol{v}_G - mg\,(h\,\mathrm{c}_\varphi - \Delta h_G) \tag{10}$$

To calculate the mass center velocity, we take a similar approach as in (9) and obtain

$$\boldsymbol{v}_G = (v_{rx} - h\dot{\psi}\,\mathrm{s}_\varphi)\boldsymbol{i} + (v_{ry} + b\dot{\psi} + h\dot{\varphi}\,\mathrm{c}_\varphi)\boldsymbol{j} + h\dot{\varphi}\,\mathrm{s}_\varphi\,\boldsymbol{k}.$$

Plugging the above equations and (4)-(7) into (10), we obtain

$$\begin{aligned} L = \frac{J_s}{2\,\mathrm{c}_\xi^2}\dot{\sigma}^2 + \frac{1}{2}m\big[(v_{rx} - h\dot{\psi}\,\mathrm{s}_\varphi)^2 + (v_{ry} + b\dot{\psi} + h\dot{\varphi}\,\mathrm{c}_\varphi)^2 + \\ h^2\dot{\varphi}^2\,\mathrm{s}_\varphi^2\big] - mg\left(h\,\mathrm{c}_\varphi - \frac{bl_t\,\mathrm{c}_\xi}{l}\sigma\,\mathrm{s}_\varphi\right). \end{aligned} \tag{11}$$

Incorporating the constraints (6), we obtain the constrained Lagrangian L_c as [2]

$$\begin{aligned} L_c = \frac{J_s}{2\,\mathrm{c}_\xi^2}\,\mathrm{c}_\varphi^2\,\dot{\sigma}^2 + \frac{1}{2}m\Bigg\{\left[\left(1 - \frac{h}{l}\sigma\,\mathrm{s}_\varphi\right)^2 + \frac{b^2}{l^2}\sigma^2\right]v_{rx}^2 \\ + v_{ry}^2 + \frac{2b}{l}\sigma v_{rx}v_{ry} + \frac{2bh}{l}\,\mathrm{c}_\varphi\,\sigma\dot{\varphi}v_{rx} + 2h\,\mathrm{c}_\varphi\,\dot{\varphi}v_{ry} \\ + h^2\dot{\varphi}^2\Bigg\} - mg\left(h\,\mathrm{c}_\varphi - \frac{bl_t\,\mathrm{c}_\xi}{l}\sigma\,\mathrm{s}_\varphi\right). \end{aligned} \tag{12}$$

The moment M_s on the rotating axis is obtained as

$$M_s = \frac{l_t}{\sqrt{1 + (l_t/r)^2}}\left(F_{fy}\,\mathrm{c}_{\varphi_f} - F_{fz}\,\mathrm{s}_{\varphi_f}\right). \tag{13}$$

The detailed calculation of (13) is given in Appendix I.

The equations of motion using the constrained Lagrangian are obtained as [24] [3]

$$\frac{d}{dt}\frac{\partial L_c}{\partial \dot{r}^i} - \frac{\partial L_c}{\partial r^i} + A_i^k\frac{\partial L_c}{\partial s^k} = -\frac{\partial L}{\partial \dot{s}^l}C_{ij}^l\dot{r}^j + \tau^i,\ i, j = 1, \ldots, 4, \tag{14}$$

where τ^i are the external forces/torques, A_i^k is the element of connection $A(\boldsymbol{r}, \boldsymbol{s})$ at the kth row and ith column, and C_{ij}^l denote the components of the curvature of $A(\boldsymbol{r}, \boldsymbol{s})$ as

$$C_{ij}^l = \frac{\partial A_i^l}{\partial r^j} - \frac{\partial A_j^l}{\partial r^i} + A_i^k\frac{\partial A_j^l}{\partial s^k} - A_j^k\frac{\partial A_i^l}{\partial s^k}. \tag{15}$$

From state variable σ, from (14), we obtain the steering dynamics as

$$\frac{d}{dt}\left(\frac{J_s}{\mathrm{c}_\xi^2}\,\mathrm{c}_\varphi^2\,\dot{\sigma}\right) - \frac{mgl_tb\,\mathrm{c}_\xi}{l}\,\mathrm{s}_\varphi = \tau_s + M_s\,. \tag{16}$$

Considering a position feedback control of the steering angle directly, we can reduce the dynamic equation (16) by a kinematic steering system as

$$\dot{\sigma} = \omega_\sigma, \tag{17}$$

where the input ω_σ is considered as the virtual steering velocity and given by dynamic extension

$$\dot{\omega}_\sigma = \frac{\mathrm{c}_\xi^2}{J_s\,\mathrm{c}_\varphi^2}\,(\tau_s + M_s) - 2\tan\varphi\dot{\varphi}\dot{\sigma} + \frac{mgl_tb\,\mathrm{c}_\xi^3}{lJ_s}\,\mathrm{s}_\varphi\,.$$

Similarly, we obtain the roll dynamics equation

$$\begin{aligned} \frac{bh\sigma}{l}\mathrm{c}_\varphi\,\dot{v}_{rx} + h\,\mathrm{c}_\varphi\,\dot{v}_{ry} + h^2\ddot{\varphi} + \left(1 - \frac{h\sigma}{l}\,\mathrm{s}_\varphi\right)\frac{h\sigma\,\mathrm{c}_\varphi}{l}v_{rx}^2 \\ - g\left(h\,\mathrm{s}_\varphi + \frac{l_tb\,\mathrm{c}_\xi}{l}\sigma\,\mathrm{c}_\varphi\right) = -\frac{bh}{l}\,\mathrm{c}_\varphi\,v_{rx}\omega_\sigma, \end{aligned} \tag{18}$$

[2] Readers can refer to [24] for the definition of the constrained Lagrangian L_c and also Chapter 5 of [24] for the Lagrange-d'Alembert principle for nonholonomic constrained dynamical systems.

[3] Here the summation convention is used where, for example, if s is of dimension m, then $A_i^k\frac{\partial A_j^l}{\partial s^k} \equiv \Sigma_{k=1}^m A_i^k\frac{\partial A_j^l}{\partial s^k}$.

Preprint submitted to 48th IEEE Conference on Decision and Control.
Received March 5, 2009.

longitudinal dynamics equation

$$\left[\left(1-\frac{h\sigma}{l}\,\mathrm{s}_\varphi\right)^2+\frac{b^2\sigma^2}{l^2}\right]\dot{v}_{rx}+\frac{b\sigma}{l}\dot{v}_{ry}+\frac{bh\sigma}{l}\,\mathrm{c}_\varphi\,\ddot{\varphi}-2\Big(1-\frac{h\sigma}{l}\,\mathrm{s}_\varphi\Big)\frac{h\sigma}{l}\,\mathrm{c}_\varphi\,\dot{\varphi}v_{rx}-\frac{bh\sigma}{l}\,\mathrm{s}_\varphi\,\dot{\varphi}^2=-\Big[-2\Big(1-\frac{h\sigma}{l}\,\mathrm{s}_\varphi\Big)\frac{h}{l}\,\mathrm{s}_\varphi\,v_{rx}+\frac{2b^2\sigma}{l^2}v_{rx}+\frac{b}{l}v_{ry}+\frac{bh}{l}\,\mathrm{c}_\varphi\,\dot{\varphi}\Big]\omega_\sigma+\frac{1}{m}F_{rx}-\frac{1}{m\sqrt{1+\sigma^2}}\left(F_{fx}+\sigma F_{fy}\right)-\frac{1}{m}C_d v_{rx}^2, \tag{19}$$

and lateral dynamics equation

$$\frac{b\sigma}{l}\dot{v}_{rx}+\dot{v}_{ry}+h\,\mathrm{c}_\varphi\,\ddot{\varphi}-h\,\mathrm{s}_\varphi\,\dot{\varphi}^2=-\frac{bv_{rx}}{l}\omega_\sigma-\frac{1}{m}F_{ry}+\frac{1}{m\sqrt{1+\sigma^2}}\left(F_{fy}-\sigma F_{fx}\right). \tag{20}$$

In (19), C_d is the aerodynamic drag coefficient.

Let $\dot{\boldsymbol{q}} := [\dot{\varphi}\ \ v_{rx}\ \ v_{ry}]^T$ denote the generalized velocity of the motorcycle and we rewrite the above dynamics equations (18)-(20) in a compact matrix form as

$$\mathbf{M}\ddot{\boldsymbol{q}}=\mathbf{K}_m+\mathbf{B}_m\begin{bmatrix}\omega_\sigma\\F_{fx}\\F_{fy}\\F_{rx}\\F_{ry}\end{bmatrix}, \tag{21}$$

where matrices

$$\mathbf{M}=\begin{bmatrix}M_{11}&M_{12}\\M_{21}&M_{22}\end{bmatrix}=\left[\begin{array}{c|cc}h^2&\frac{bh\sigma}{l}\,\mathrm{c}_\varphi&h\,\mathrm{c}_\varphi\\\hline\frac{bh\sigma}{l}\,\mathrm{c}_\varphi&\left(1-\frac{h\sigma}{l}\,\mathrm{s}_\varphi\right)^2+\frac{b^2\sigma^2}{l^2}&\frac{b\sigma}{l}\\h\,\mathrm{c}_\varphi&\frac{b\sigma}{l}&1\end{array}\right],$$

$$\mathbf{K}_m=\begin{bmatrix}-\left(1-\frac{h\sigma}{l}\,\mathrm{s}_\varphi\right)\frac{h\sigma\,\mathrm{c}_\varphi}{l}v_{rx}^2+g\left(h\,\mathrm{s}_\varphi+\frac{l_t b\,\mathrm{c}_\xi}{l}\sigma\,\mathrm{c}_\varphi\right)\\2\left(1-\frac{h\sigma}{l}\,\mathrm{s}_\varphi\right)\frac{h\sigma}{l}\,\mathrm{c}_\varphi\,\dot{\varphi}v_{rx}+\frac{bh\sigma}{l}\,\mathrm{s}_\varphi\,\dot{\varphi}^2-\frac{1}{m}C_d v_{rx}^2\\h\,\mathrm{s}_\varphi\,\dot{\varphi}^2\end{bmatrix},$$

and

$$\mathbf{B}_m=\begin{bmatrix}-\frac{bh}{l}\,\mathrm{c}_\varphi\,v_{rx}&0&0&0&0\\B_\omega&-\frac{1}{m\sqrt{1+\sigma^2}}&-\frac{\sigma}{m\sqrt{1+\sigma^2}}&\frac{1}{m}&0\\-\frac{bv_{rx}}{l}&-\frac{\sigma}{m\sqrt{1+\sigma^2}}&\frac{1}{m\sqrt{1+\sigma^2}}&0&-\frac{1}{m}\end{bmatrix}.$$

In the above matrix $\mathbf{B}_m$,

$$B_\omega=2\left[\left(1-\frac{h\sigma}{l}\,\mathrm{s}_\varphi\right)\frac{h}{l}\,\mathrm{s}_\varphi-\frac{b^2\sigma}{l^2}\right]v_{rx}-\frac{b}{l}v_{ry}-\frac{bh}{l}\,\mathrm{c}_\varphi\,\dot{\varphi}.$$

It is clear that the control inputs in (17) and (21) are the virtual steering velocity ω_σ and the wheel traction/braking forces $\boldsymbol{F}_f$ and $\boldsymbol{F}_r$.

IV. Tire Dynamics Models

In this section, we discuss how to capture the motorcycle tire/road interaction. We particularly like to present a friction forces modeling scheme for motorcycle dynamics (21).

A. Tire kinematics relationships

Fig. 3 illustrates the kinematics of the tire/road contact. Let $\boldsymbol{v}_c=v_{cx}\boldsymbol{i}+v_{cy}\boldsymbol{j}+v_{cz}\boldsymbol{k}$ and $\boldsymbol{v}_o=v_{ox}\boldsymbol{i}+v_{oy}\boldsymbol{j}+v_{oz}\boldsymbol{k}$ denote the velocities of the contact point and the wheel center in the frame $\mathcal{B}$, respectively. We define the longitudinal slip ratio λ_s and lateral side slip ratio λ_γ, respectively, as

$$\lambda_s:=\frac{v_{cx}-r\omega_w}{v_{cx}},\ \lambda_\gamma:=\tan\gamma=-\frac{v_{cy}}{v_{cx}}, \tag{22}$$

where ω_w is the wheel angular velocity.

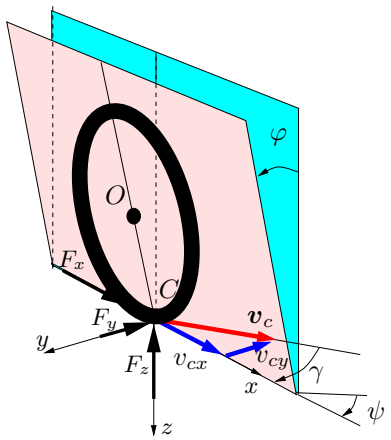

Fig. 3. Schematic of the tire kinematics.

For the front wheel, the camber angle is different (8), and the velocity relationship between C_1 and the wheel center O_1 in $\mathcal{B}$ is then

$$v_{fx}=v_{fox}+r\dot{\psi}\,\mathrm{s}_\varphi,\ v_{fcy}=v_{foy}-r\dot{\varphi}_f\,\mathrm{c}_\varphi,\quad v_{fz}=v_{foz}-r\dot{\varphi}_f\,\mathrm{s}_\varphi. \tag{23}$$

Using the relationship (9) and (8), we simplify the above velocity calculation and obtain

$$v_{fx}=v_{rx},\ v_{fy}=v_{ry}-r\dot{\phi}\,\mathrm{s}_\xi\,\mathrm{c}_\varphi+l\dot{\psi}. \tag{24}$$

From the side slip ratio (22) of the rear wheel, we have

$$\lambda_{r\gamma}=\tan\gamma_r=-\frac{v_{ry}}{v_{rx}}=-\frac{v_{fy}}{v_{fx}}-\frac{r\dot{\phi}\,\mathrm{s}_\xi\,\mathrm{c}_\varphi-l\dot{\psi}}{v_{rx}}=\tan\gamma_f'-\frac{r\tan\xi\,\mathrm{c}_\varphi^2}{v_{rx}}\omega_\sigma+\sigma, \tag{25}$$

where $\gamma_f':=\phi_g-\gamma_f$ and $\tan\gamma_f'=-\frac{v_{fy}}{v_{fx}}$; see Fig. 2. We also use relationships (4) and (5) in the last step above. Moreover, from (2) and the geometry and kinematics of the front wheel (Fig. 2), we have

$$\sigma=\tan\phi_g=\tan(\gamma_f'+\gamma_f)\approx\tan\gamma_f'+\tan\gamma_f=\lambda_{r\gamma}+\frac{r\tan\xi\,\mathrm{c}_\varphi^2}{v_{rx}}\omega_\sigma-\sigma+\lambda_{f\gamma}.$$

Therefore, we obtain the relationship between the front and rear wheel side slip ratios as follows.

$$\lambda_{f\gamma}=2\sigma-\frac{r\tan\xi\,\mathrm{c}_\varphi^2}{v_{rx}}\omega_\sigma-\lambda_{r\gamma}. \tag{26}$$

Preprint submitted to 48th IEEE Conference on Decision and Control.
Received March 5, 2009.

Similarly, we can obtain the slip ratio calculation of the front wheel as follows. First, we obtain the longitudinal velocity of the contact point C_1 as

$$v_{fx_w} = v_{fx}\,\mathrm{c}_{\phi_g} + v_{fy}\,\mathrm{s}_{\phi_g} \approx v_{rx}\,\mathrm{c}_{\phi_g} + (v_{ry} + \sigma v_{rx})\,\mathrm{s}_{\phi_g} = \frac{1}{\sqrt{1+\sigma^2}}\left[\left(1+\sigma^2\right)v_{rx} + \sigma v_{ry}\right].$$

Therefore, by the definition (22), we obtain the front wheel longitudinal slip ratio

$$\lambda_{fs} = 1 - \frac{r\omega_f}{v_{fx_w}} = 1 - \frac{r\sqrt{1+\sigma^2}}{(1+\sigma^2)v_{rx} + \sigma v_{ry}}\omega_f. \tag{27}$$

B. Modeling of frictional forces

Modeling of the frictional forces between the tire and the road surface is complex. Here we focus on modeling of the longitudinal force F_x and lateral force F_y because of their importance in motorcycle dynamics and control.

The tire/road frictional forces depend on many factors, such as slip and slip angles, vehicle velocity, normal load, and tire and road conditions, etc. It is widely accepted that the pseudo-static relationships, namely, the mathematical models of the longitudinal force F_x and slip λ, and the lateral force F_y and slip angle γ, are the most useful characteristics to capture the tire/road interaction. To capture tire/road friction characteristics, we propose to approximate the friction forces by a piecewise linear relationship shown in Fig. 4. Let $F(x)$ denote the frictional force as a function of independent variable x. The piecewise linear function $F(x)$ captures the property of the tire/road forces: when $0 \le x \le x_m$, $F(x) = kx$, and when $x_m < x \le x_{\max}$, $F = \frac{(1-\alpha_x)F_m}{x_m - x_{\max}}(x - x_m) + F_m$, where $0 \le \alpha_x \le 1$ is a constant that denotes the fraction of the force at $x_{\max}$ of the maximum force F_m. We can write the force $F(x)$ as follows.

$$F(x) = k(a_1 + a_2 x), \tag{28}$$

where

$$a_1 = \begin{cases} 0 & 0 \le x \le x_m \\ \frac{(x_{\max} - x_m)x_m}{x_{\max} - x_m} & x_m < x \le x_{\max} \end{cases}$$

and

$$a_2 = \begin{cases} 1 & 0 \le x \le x_m \\ \frac{-(1-\alpha_x)x_m}{x_{\max} - x_m} & x_m < x \le x_{\max} \end{cases}$$

With the force model (28), we can write the longitudinal force as

$$F_x(\lambda_s) = k_\lambda\left[a_{1\lambda} + a_{2\lambda}\,\mathrm{sign}(\lambda_s)\lambda_s\right], \tag{29}$$

where the function $\mathrm{sign}(x) = 1$ for $x \ge 0$ and -1 otherwise is used to capture both positive (braking) and negative (traction) forces for $F_x(\lambda_s)$. For the lateral force, due to the large camber angle of the motorcycle tires, we have

$$F_y(\lambda_{eq}) = k_\gamma\left[a_{1\gamma} + a_{2\gamma}\,\mathrm{sign}(\lambda_{eq})\lambda_{eq}\right], \tag{30}$$

where we define the equivalent side slip ratio

$$\lambda_{eq} = \tan\gamma_{eq} = \tan\left(\gamma + \frac{k_\varphi}{k_\gamma}\varphi\right) \approx \lambda_\gamma + \frac{k_\varphi}{k_\gamma}\tan\varphi.$$

The values of the longitudinal, corning, and cambering coefficients, k_λ, k_γ, k_φ, depend on the normal load F_z. Due to the acceleration and deceleration, the normal load F_z is changing during motion. For front and rear wheels, the normal loads F_{fz} and F_{rz} are obtained respectively as

$$F_{fz} = \frac{b}{l}mg - \frac{h}{l}m\dot{v}_{Gx},\ F_{rz} = \frac{l-b}{l}mg + \frac{h}{l}m\dot{v}_{Gx}, \tag{31}$$

where $\dot{v}_{Gx}$ is the longitudinal acceleration of the motorcycle at the mass center G. The relationship between $\dot{v}_{Gx}$ and the acceleration of point C_2 is obtained as

$$\dot{v}_{Gx} = \dot{v}_{rx} - v_{ry}\dot{\psi} - h\ddot{\psi}\,\mathrm{s}_\varphi - b\dot{\psi}^2 - 2h\dot{\psi}\dot{\varphi}\,\mathrm{c}_\varphi\,.$$

The calculation of the above relationship is given in Appendix II. In this paper, we use the tire models in [25] to calculate the dependence of the stiffness coefficients on the normal load.

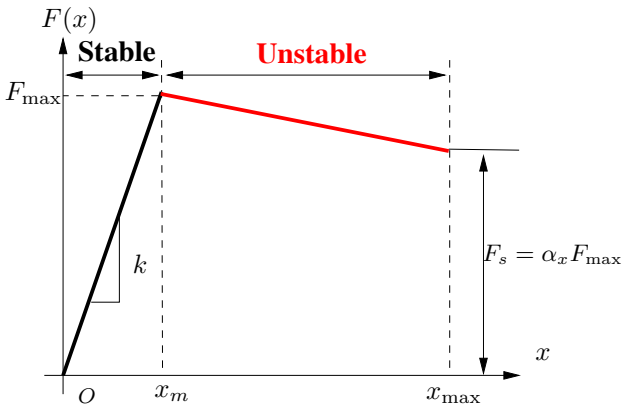

Fig. 4. Linear approximation of the tire/road frictional force $F(x)$.

C. Combined tire and motorcycle dynamics models

We combine the motorcycle dynamics (17) and (21) with the tire dynamics. The controlled input variables are the front and rear wheel angular velocities, namely, ω_f and ω_r, respectively, and the steering angle ϕ. Note that the driving wheel is the rear wheel and we can only apply braking for the front wheel, namely, $F_{fx} \ge 0$. For the control system design, we consider the pseudo-static friction models (29) and (30), and therefore we write the longitudinal at the front and rear wheels as

$$F_{fx} = F_{1f} + F_{2f}\lambda_{fs},\quad F_{rx} = F_{1r} + F_{2r}\lambda_{rs} \tag{32}$$

and lateral forces

$$F_{fy} = F_{3f} + F_{4f}\left(\lambda_{f\gamma} + \frac{k_{f\varphi}}{k_{f\gamma}}\tan\varphi_f\right),$$
$$F_{ry} = F_{3r} + F_{4r}\left(\lambda_{r\gamma} + \frac{k_{r\varphi}}{k_{r\gamma}}\tan\varphi\right), \tag{33}$$

where $F_{1i} = k_{i\lambda}a_{1i\lambda}$, $F_{2i} = k_{i\lambda}a_{2i\lambda}\,\mathrm{sign}(\lambda_{is})$, $F_{1i} = k_{i\lambda}a_{1i\lambda}$, $F_{2i} = k_{i\lambda}a_{2i\lambda}\,\mathrm{sign}(\lambda_{is})$, $i = f, r$, and $a_{ji\lambda}$, $a_{ji\gamma}$, $j = 1, 2$, are the longitudinal and lateral force model parameters defined in (28), respectively.

Plugging (32) and (33) into (21) and using the relationship (26), we obtain

$$\mathbf{M}(\boldsymbol{q},\sigma)\ddot{\boldsymbol{q}} = \mathbf{K}(\dot{\boldsymbol{q}},\boldsymbol{q},\sigma) + \mathbf{B}\boldsymbol{u}, \tag{34}$$

Preprint submitted to 48th IEEE Conference on Decision and Control.
Received March 5, 2009.

where input $\boldsymbol{u} := \begin{bmatrix}\omega_\sigma & \boldsymbol{u}_\lambda^T\end{bmatrix}^T$, $\boldsymbol{u}_\lambda = \begin{bmatrix}\lambda_{fs} & \lambda_{rs}\end{bmatrix}^T$, matrix

$$\mathbf{K} = \begin{bmatrix} K_1 \\ \hdashline K_2 \end{bmatrix} = \begin{bmatrix} (K_m)_1 \\ \hdashline (K_m)_2 - \dfrac{F_{1f}}{m\sqrt{1+\sigma^2}} - \dfrac{\sigma}{m\sqrt{1+\sigma^2}} F_{34} + \dfrac{F_{1r}}{m} \\ (K_m)_3 - \dfrac{\sigma F_{1f}}{m\sqrt{1+\sigma^2}} + \dfrac{1}{m\sqrt{1+\sigma^2}} F_{34} - \dfrac{F_{ry}}{m} \end{bmatrix},$$

$(K_m)_i$ is the ith row of matrix $\mathbf{K}$, $F_{34} = F_{3f} + F_{4f}\left(\lambda_{f\gamma} + \frac{k_{f\varphi}}{k_{f\gamma}}(2\sigma - \lambda_{r\gamma})\right)$, and

$$\mathbf{B} = \begin{bmatrix} B_{11} & B_{12} \\ \hdashline B_{21} & B_{22} \end{bmatrix} = \left[\begin{array}{c:cc} -\dfrac{bh}{l}\,\mathrm{c}_\varphi\, v_{rx} & 0 & 0 \\ \hdashline B_\omega + \dfrac{r\sigma F_{4f}\tan\xi\,\mathrm{c}_\varphi^2\, k_{f\varphi}}{m v_{rx} k_{f\gamma}\sqrt{1+\sigma^2}} & -\dfrac{F_{2f}}{m\sqrt{1+\sigma^2}} & \dfrac{F_{2r}}{m} \\ -\dfrac{b v_{rx}}{l} - \dfrac{r F_{4f}\tan\xi\,\mathrm{c}_\varphi^2\, k_{f\varphi}}{m v_{rx} k_{f\gamma}\sqrt{1+\sigma^2}} & -\dfrac{\sigma F_{2f}}{m\sqrt{1+\sigma^2}} & 0 \end{array}\right].$$

In the companion paper [3], we will develop a trajectory tracking and balancing control for dynamics (34).

V. Conclusion

In this paper, we presented a new nonlinear dynamic model for autonomous motorcycles. The proposed model is obtained through a contrained Lagrange modeling approach. The new features of the proposed motorcycle dynamics are twofold: First, we relaxed the assumption of zero-lateral-velocity constraints at tire contact points and thus the model can be used for the agile maneuvers when wheels run with large longitudinal slips and lateral side slips. Second, we considered the motorcycle tire models and extended previously developed motorcycle dynamics. The control inputs for the proposed motorcycle dynamics are the front wheel steering angle and the angular velocities for the front and rear wheels. The trajectory tracking and balance control systems design is based on the new dynamic model and presented in the companion paper [3].

Currently, we plan to extend the motorcycle dynamics models in two directions. First, we will relax the neutral driving approximation and present a general yaw dynamics model. Second, a coupled longitudinal and lateral motorcycle tire dynamics will be developed and the LuGre dynamic friction model is currently used to capture the coupled tire/road friction characteristics.

Acknowledgments

The first author thanks Dr. N. Getz at Inversion Inc. for his helpful suggestions and support. The authors are grateful to Prof. S. Jayasuriya at Texas A&M University, Dr. E.H. Tseng and Dr. J. Lu at Ford Research and Innovation Center for their helpful discussions and suggestions.

References

[1] A. Levandowski, A. Schultz, C. Smart, A. Krasnov, H. Chau, B. Majusiak, F. Wang, D. Song, J. Yi, H. Lee, and A. Parish, "Ghostrider: Autonomous motorcycle," in *Proc. IEEE Int. Conf. Robot. Automation (Video)*, Orlando, FL, 2006.

[2] D. Limebeer and R. Sharp, "Bicycles, motorcycles, and models," *IEEE Control Syst. Mag.*, vol. 26, no. 5, pp. 34–61, 2006.

[3] J. Yi, Y. Zhang, and D. Song, "Autonomous motorcycles for agile maneuvers: Part II: Control systems design," *Submitted to the 48th IEEE Conf. on Decision and Control*.

[4] N. Getz, "Dynamic inversion of nonlinear maps with applications to nonlinear control and robotics," Ph.D. dissertation, Dept. Electr. Eng. and Comp. Sci., Univ. Calif., Berkeley, CA, 1995.

[5] J. Yi, D. Song, A. Levandowski, and S. Jayasuriya, "Trajectory tracking and balance stabilization control of autonomous motorcycles," in *Proc. IEEE Int. Conf. Robot. Autom.*, Orlando, FL, 2006, pp. 2583–2589.

[6] K. Åström, R. Klein, and A. Lennartsson, "Bicycle dynamics and control," *IEEE Control Syst. Mag.*, vol. 25, no. 4, pp. 26–47, 2005.

[7] J. Lowell and H. McKell, "The stability of bicycles," *Amer. J. Phys.*, vol. 50, no. 12, pp. 1106–1112, 1982.

[8] R. Sharp, "Stability, control and steering responses of motorcycles," *Veh. Syst. Dyn.*, vol. 35, no. 4-5, pp. 291–318, 2001.

[9] V. Cossalter and R. Lot, "A motorcycle multi-body model for real time simulations based on the natural coordinates approach," *Veh. Syst. Dyn.*, vol. 37, no. 6, pp. 423–447, 2002.

[10] V. Cossalter, *Motorcycle Dynamics*. Greendale, WI: Race Dynamics, 2002.

[11] P. Kessler, "Motorcycle navigation with two sensors," Master's thesis, Dept. Mech. Eng., Univ. California, Berkeley, CA, 2004.

[12] R. Sharp, "The stability and control of motorcycles," *J. Mech. Eng. Sci.*, vol. 13, no. 5, pp. 316–329, 1971.

[13] F. Biral, D. Bortoluzzi, V. Cossalter, and M. Da Lio, "Experimental study of motorcycle transfer functions for evaluating handling," *Veh. Syst. Dyn.*, vol. 39, no. 1, pp. 1–25, 2003.

[14] D. Jones, "The stability of the bicycle," *Physics Today*, vol. 23, no. 4, pp. 34–40, 1970.

[15] J. Fajans, "Steering in bicycles and motorcycles," *Amer. J. Phys.*, vol. 68, no. 7, pp. 654–659, 2000.

[16] V. Cossalter, R. Lot, and F. Maggio, "The modal analysis of a motorcycle in straight running and on a curve," *Meccanica*, vol. 39, pp. 1–16, 2004.

[17] J. Meijaard, J. Papadopoulos, A. Ruina, and A. Schwab, "Linearized dynamics equations for the balance and steer of a bicycle: A benchmark and review," *Proc. Royal Soc. A*, vol. 463, pp. 1955–1982, 2007.

[18] A. Beznos and A. Formal'sky and E. Gurfinkel and D. Jicharev and A. Lensky and K. Savitsky and L. Tchesalin, "Control of autonomous motion of two-wheel bicycle with gyroscopic stabilisation," in *Proc. IEEE Int. Conf. Robot. Autom.*, Leuven, Belgium, 1998, pp. 2670–2675.

[19] S. Lee and W. Ham, "Self-stabilzing strategy in tracking control of unmanned electric bicycle with mass balance," in *Proc. IEEE/RSJ Int. Conf. Intell. Robot. Syst.*, Lausanne, Switzerland, 2002, pp. 2200–2205.

[20] Y. Tanaka and T. Murakami, "Self sustaining bicycle robot with steering controller," in *Proc. 2004 IEEE Adv. Motion Contr. Conf.*, Kawasaki, Japan, 2004, pp. 193–197.

[21] ——, "A study on straight-line tracking and posture control in electric bicycle," *IEEE Trans. Ind. Electron.*, vol. 56, no. 1, pp. 159–168, 2009.

[22] R. Lot, "A motorcycle tires model for dynamic simulations : Theoretical and experimental aspects," *Meccanica*, vol. 39, pp. 207–220, 2004.

[23] J. Hauser and A. Saccon, "Motorcycle modeling for high-performance maneuvering," *IEEE Control Syst. Mag.*, vol. 26, no. 5, pp. 89–105, 2006.

[24] A. Bloch, *Nonholonomic Mechanics and Control*. New York, NY: Springer, 2003.

[25] R. S. Sharp, S. Evangelou, and D. J. N. Limbeer, "Advances in the modelling of motorcycle dynamics," *Multibody Syst. Dyn.*, vol. 12, pp. 251–283, 2004.

Appendix I
Calculation of M_s

We consider the front wheel center O_1 and the projected steering axis point C_3 on the ground surface. Since the

frictional moment is independent of the coordinate system. We can setup a local coordinate system $x_f y_f z_f$ by rotating the coordinate system xyz around the z-axis with an angle ϕ_g (origin at contact point C_1). Let $(\boldsymbol{i}_f, \boldsymbol{i}_f, \boldsymbol{i}_f)$ denote the unit vectors along the x_f, y_f, z_f-axis directions, respectively.

In the new coordinate system, we obtain the coordinates of O_1 and C_3 as $(0, r\,\mathrm{s}_{\varphi_f}, -r\,\mathrm{c}_{\varphi_f})$ and $(l_t, 0, 0)$, respectively. We write the front wheel friction force vector $\boldsymbol{F}_f$ as

$$\boldsymbol{F}_f = -F_{fx}\boldsymbol{i}_f - F_{fy}\boldsymbol{j}_f - F_{fz}\boldsymbol{k}_f$$

and the vector $\boldsymbol{r}_{C_3C_1} = -l_t\boldsymbol{i}_f$. The directional vector $\boldsymbol{n}_{O_1C_3}$ of the steering axis O_1, C_3 is then

$$\boldsymbol{n}_{O_1C_3} = \frac{l_t\boldsymbol{i}_f - r\,\mathrm{s}_{\varphi_f}\,\boldsymbol{j}_f + r\,\mathrm{c}_{\varphi_f}\,\boldsymbol{k}_f}{\sqrt{l_t^2 + r^2}}.$$

Therefore, the friction moment M_s about the steering axis is calculated as

$$\begin{aligned} M_s &= (\boldsymbol{r}_{C_3C_1} \times \boldsymbol{F}_f) \cdot \boldsymbol{n}_{O_1C_3} \\ &= \frac{l_t}{\sqrt{1 + (l_t/r)^2}} \left(F_{fy}\,\mathrm{c}_{\varphi_f} - F_{fz}\,\mathrm{s}_{\varphi_f}\right). \end{aligned}$$

APPENDIX II
CALCULATION OF ACCELERATION $\dot{\boldsymbol{v}}_G$

Taking the time derivative of the mass center velocity $\boldsymbol{v}_G$ and considering the moving frame xyz's angular velocity $\boldsymbol{\omega} = \dot{\varphi}\boldsymbol{i} + \dot{\psi}\boldsymbol{k}$, we obtain

$$\begin{aligned} \dot{\boldsymbol{v}}_G = \frac{\delta \boldsymbol{v}_G}{\delta t} + \boldsymbol{\omega} \times \boldsymbol{v}_G &= (\dot{v}_{rx} - h\ddot{\psi}\,\mathrm{s}_\varphi - h\dot{\psi}\dot{\varphi}\,\mathrm{c}_\varphi)\boldsymbol{i} + \\ &(\dot{v}_{ry} + b\ddot{\psi} + h\ddot{\varphi}\,\mathrm{c}_\varphi - h\dot{\varphi}^2\,\mathrm{s}_\varphi)\boldsymbol{j} + (h\ddot{\varphi}\,\mathrm{s}_\varphi + h\dot{\varphi}^2\,\mathrm{c}_\varphi)\boldsymbol{k} \\ &+ (\dot{\varphi}\boldsymbol{i} + \dot{\psi}\boldsymbol{k}) \times \boldsymbol{v}_G \\ = (\dot{v}_{rx} - v_{ry}\dot{\psi} - h\ddot{\psi}\,\mathrm{s}_\varphi - b\dot{\psi}^2 - 2h\dot{\psi}\dot{\varphi}\,\mathrm{c}_\varphi)\boldsymbol{i} &+ (\dot{v}_{ry} + \\ v_{rx}\dot{\psi} + b\ddot{\psi} + h\ddot{\varphi}\,\mathrm{c}_\varphi - h\dot{\psi}^2\,\mathrm{s}_\varphi - 2h\dot{\varphi}^2\,\mathrm{s}_\varphi)\boldsymbol{j} &+ (v_{ry}\dot{\varphi} + \\ h\ddot{\varphi}\,\mathrm{s}_\varphi + b\dot{\psi}\dot{\varphi} + 2h\dot{\varphi}^2\,\mathrm{c}_\varphi)\boldsymbol{k}, \end{aligned}$$

where $\frac{\delta \boldsymbol{v}_G}{\delta t}$ denotes the derivative of $\boldsymbol{v}_G$ by treating the xyz-coordinate as a fixed frame.

Preprint submitted to 48th IEEE Conference on Decision and Control.
Received March 5, 2009.